Identification of the Oxygen Activation Site in Monomeric Sarcosine Oxidase: Role of Lys265 in Catalysis[†]

Guohua Zhao, Robert C. Bruckner, and Marilyn Schuman Jorns*

Department of Biochemistry and Molecular Biology, Drexel University College of Medicine, Philadelphia, Pennsylvania 19102

Received May 11, 2008; Revised Manuscript Received June 26, 2008

ABSTRACT: Monomeric sarcosine oxidase (MSOX) catalyzes the oxidation of *N*-methylglycine and contains covalently bound FAD that is hydrogen bonded at position N(5) to Lys265 via a bridging water. Lys265 is absent in the homologous but oxygen-unreactive FAD site in heterotetrameric sarcosine oxidase. Isolated preparations of Lys265 mutants contain little or no flavin but can be covalently reconstituted with FAD. Mutation of Lys265 to a neutral residue (Ala, Gln, Met) causes a 6000- to 9000-fold decrease in apparent turnover rate whereas a 170-fold decrease is found with Lys265Arg. Substitution of Lys265 with Met or Arg causes only a modest decrease in the rate of sarcosine oxidation (9.0- or 3.8-fold, respectively), as judged by reductive half-reaction studies which show that the reactions proceed via an initial enzyme·sarcosine charge transfer complex and a novel spectral intermediate not detected with wild-type MSOX. Oxidation of reduced wild-type MSOX ($k = 2.83 \times 10^5$ M^{-1} s^{-1}) is more than 1000-fold faster than observed for the reaction of oxygen with free reduced flavin. Mutation of Lys265 to a neutral residue causes a dramatic 8000-fold decrease in oxygen reactivity whereas a 250-fold decrease is observed with Lys265Arg. The results provide definitive evidence for Lys265 as the site of oxygen activation and show that a single positively charged amino acid residue is entirely responsible for the rate acceleration observed with wild-type enzyme. Significantly, the active sites for sarcosine oxidation and oxygen reduction are located on opposite faces of the flavin ring.

The reduction of oxygen to hydrogen peroxide by free reduced flavin is thermodynamically favorable but kinetically slow because the 2-electron reduction of triplet oxygen by a diamagnetic organic molecule is spin-forbidden. In fact, the 2-electron reduction of oxygen by reduced flavin proceeds via an initial 1-electron transfer step that generates a flavin radical/superoxide anion radical pair in a spin-allowed but energetically unfavorable, rate-determining reaction. The term oxygen activation is used in reference to the accelerated rates of oxygen reduction observed with flavoprotein oxidases and other enzymes that reduce molecular oxygen (*1, 2*). A series of elegant studies by Klinman and Roth identified His516 as the site of oxygen activation in the flavoenzyme glucose oxidase and showed that the reaction required the protonated form of this residue (*2–4*). Surprisingly little is, however, currently known about the detailed mechanism of oxygen activation by other flavoprotein oxidases, especially regarding the specific role of active site residues in these reactions.

We have initiated studies with monomeric sarcosine oxidase (MSOX[1]) in order to further explore the mechanism of oxygen activation by flavoprotein oxidases. MSOX is a stable, readily expressed 44 kDa two-domain protein that contains covalently bound FAD (8α-S-cysteinyl-FAD). The enzyme catalyzes the oxidation of sarcosine (*N*-methylglycine) and other secondary amino acids to the corresponding imines. Steady-state kinetic studies indicate that the reduced enzyme·imine product complex is the species that reacts with oxygen to generate oxidized enzyme and hydrogen peroxide (*5–7*). Recent studies indicate that covalent flavinylation of apoMSOX proceeds via an autocatalytic reaction that involves formation of an oxygen-reactive reduced flavin intermediate, covalently bound 1,5-dihydroFAD (*8–10*). High-resolution crystal structures of the MSOX holoenzyme show that the flavin ring of FAD is bound at the interface between the flavin domain and the catalytic domain. The site of sarcosine oxidation is located just above the *re*-face of the flavin ring. Access to the active site is controlled by a loop (Gly56 to Glu60) that forms part of a cleft leading from the surface. The active site loop is mobile in the free enzyme but assumes a closed conformation in enzyme complexes with competitive inhibitors (*6, 11, 12*).

MSOX is a prototypical member of a family of monomeric amino acid oxidases that contain covalently bound flavin, including *N*-methyltryptophan oxidase, nikD, pipecolate oxidase and fructosyl amino acid oxidase (*13–18*). MSOX also exhibits sequence (~20% identity) and structural (rmsd = 1.37 Å) similarity with the β-subunit of heterotetrameric sarcosine oxidase (TSOX), a bifunctional enzyme that catalyzes sarcosine oxidation and synthesis of 5,10-methylenetetrahydrofolate (*19*). The β-subunit of TSOX contains FAD which is noncovalently bound but otherwise structurally equivalent to the covalently bound FAD in MSOX. Impor-

[†] This work was supported in part by Grant GM 31704 (M.S.J.) from the National Institutes of Health.

* To whom requests for reprints should be addressed. Phone: (215) 762-7495. Fax: (215) 762-4452. E-mail: marilyn.jorns@drexelmed.edu.

[1] Abbreviations: MSOX, monomeric sarcosine oxidase; FAD, flavin adenine dinucleotide; rmsd, root-mean-square deviation; TSOX, heterotetrameric sarcosine oxidase; MTA, methylthioacetate; DMGO, dimethylglycine oxidase.

10.1021/bi8008642 CCC: $40.75
Published on Web 08/12/2008

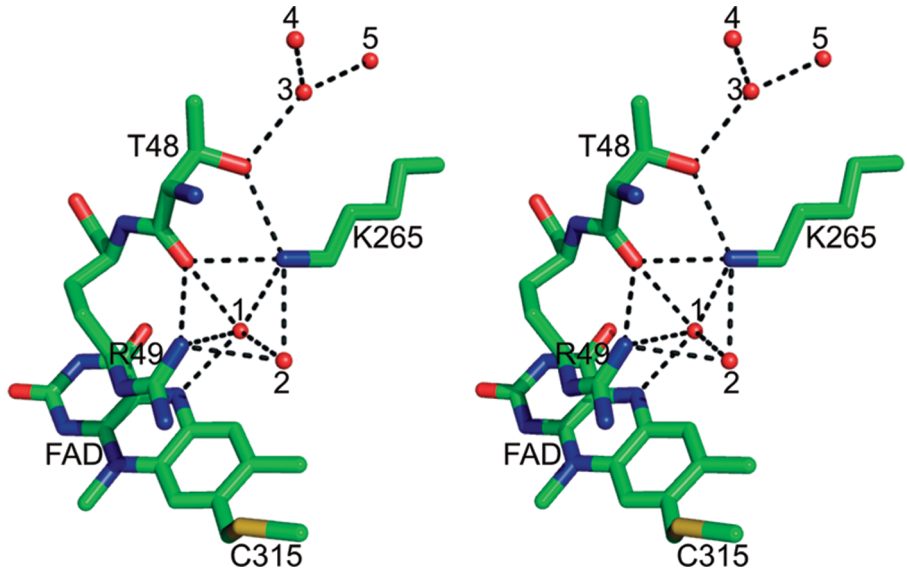

FIGURE 1: Stereoview of the region above the *si*-face of the flavin ring in wild-type MSOX (PDB code 2GBO). Carbon atoms are green, nitrogen atoms are blue, oxygen atoms are red and the sulfur atom is yellow. Active site waters are shown as balls. Waters 3−5 are in contact with bulk solvent. Hydrogen bonds are indicated by dotted lines. The diagram was rendered using PYMOL (http://www.pymol.org).

tantly, reduced FAD in TSOX is totally unreactive toward oxygen. Instead, electrons are transferred from reduced FAD to a second flavin, FMN, where oxygen is reduced to hydrogen peroxide (*20–22*). MSOX and TSOX contain highly similar sites for sarcosine oxidation above the *re*-face of FAD, as judged by structures observed for complexes of the enzymes with the same competitive inhibitor (2-furoate) (*19*). Significantly, striking differences are found above the *si*-face of FAD where two basic residues (Arg49, Lys265) are found in MSOX but absent in TSOX. The side chain of Arg49 is in van der Waals contact with the *si*-face of the flavin ring in MSOX (Figure 1), essential for covalent flavin attachment (*10*) and highly conserved in monomeric MSOX homologues that contain covalently bound FAD (*15, 23, 24*). Lys265 is hydrogen bonded to the N(5) position of the flavin ring via a bridging water (wat1) and is also hydrogen bonded to a second nearby water (wat2) (Figure 1). Lys265 is conserved in several other members of the MSOX family (*18, 23, 24*). Interestingly, a lysine residue hydrogen bonded to flavin N(5) via a bridging water is also found in a number of other flavoprotein oxidases, including monoamine oxidase B (*25*), polyamine oxidase (*26*), monoamine oxidase A (*27*), and L-amino acid oxidase (*28*). These observations suggested that Lys265 might play a role in the reaction of reduced MSOX with oxygen.

In this paper we investigate the effect of Lys265 mutations on MSOX turnover and the kinetics of the reductive- and oxidative half-reactions. The studies provide evidence for a novel intermediate during enzyme reduction and definitive evidence for Lys265 as the site of oxygen activation in MSOX.

EXPERIMENTAL PROCEDURES

Materials. Restriction enzymes and T4 DNA ligase were obtained from New England Biolabs. Plasmid pET23a was obtained from Novagen. Horseradish peroxidase and *o*-dianisidine were purchased from Sigma. Methylthioacetate was obtained from Aldrich. Talon Metal Affinity Resin (Co^{2+} affinity matrix) was obtained from Clontech. [N-methyl-D_3]-Sarcosine was obtained from Isotec.

Mutation of Lys265 to Ala, Gln, Met or Arg. Mutations were generated by using the plasmid pGZ26 (*8*) as template and the overlap extension PCR method described by Ho et al. (*29*). PCR reactions were conducted and products were purified as previously described (*10*). The left-hand fragment was generated using START (external primer) as forward primer and an internal backward primer containing the desired mutation (see Table 1). The right-hand fragment was generated using an internal forward primer containing the desired mutation and END (external primer) as backward primer. The purified left- and right-hand fragments were combined using START and END as forward and backward primers, respectively. The final PCR product was purified, digested with *Nde*I and *Xho*I, purified again and then subcloned between the *Nde*I and *Xho*I sites of plasmid pET23a. The resulting construct was used to transform *Escherichia coli* BL21(DE3) cells to ampicillin resistance. For screening, plasmid DNA was isolated from randomly selected clones and digested with *Nde*I and *Xho*I. Plasmids that exhibited the expected insert size (pGZ59, pGZ60, pGZ61, and pGZ62 for the Lys265Met, Lys265Asn, Lys265Arg and Lys265Ala mutations, respectively) were isolated and sequenced across the entire insert. Sequencing was conducted by MWG Biotech.

Expression and Purification of Wild-Type MSOX or Lys265 Mutants and Reconstitution of the Mutant Enzymes with FAD. Wild-type MSOX holoenzyme was expressed and purified as previously described (*5, 8*). The same procedure was used for expression of mutant enzymes except that the cells were grown at 23−25 °C instead of 37 °C. The mutants contained a carboxyl-terminal affinity tag, $(His)_6$, and were purified by using a Co^{2+} affinity matrix, similar to that previously described for the isolation of His-tagged wild-type MSOX apoenzyme (*8*). As will be described, the isolated preparations of the Lys265 mutants were largely or entirely devoid of covalently bound FAD. The mutant

Table 1: Primers Used for Mutagenesis[a]

primer type	forward	backward
external	START 5′-TAATACGACTCACTATAGGG-3′	END 5′-GCTAGTTATTGCTCAGCGG-3′
internal		
Lys265Ala	5′-CTGTGGATTGgcA CTAGGATATC-3′	5′-GATATCCTAGTgc CAATCCACAG-3′
Lys265Met	5′-CTGTGGATTGAtg CTAGGATATC-3′	5′-GATATCCTAGcaTCAATCCACAG-5′
Lys265Gln	5′-CTGTGGATTGcAA CTAGGATATC-3′	5′-GATATCCTAGTTg CAATCCACAG-3′
Lys265Arg	5′-CTGTGGATTGcgt CTAGGATATC-3′	5′-GATATCCTAGacg CAATCCACAG-3′

[a] Mutagenic sites in the primers are shown in lower case; the codon targeted for mutagenesis is underlined.

Table 2: Comparison of the Spectral and Catalytic Properties of Lys265 Mutants with Wild-Type MSOX[a]

	wild-type	Lys265Arg	Lys265Ala	Lys265Gln	Lys265Met
mol of covalently bound FAD/mol of protein					
untreated	0.87[b]	0.25	0.05	0	0
reconstituted		0.64	0.74	0.54	0.64
λ_{max} (nm)[c]	454, 373	449, 384	448, 386	449, 390	449, 384
ϵ_{4xy} (M^{-1} cm^{-1})[d]	12200[b]	13000	12400	12800	13500
A_{280}/A_{4xy}[d]	5.54[b]	6.62	5.93	7.73	6.53
$k_{cat_{app}}$[e] (s^{-1})	45.8 ± 0.5	0.272 ± 0.001 (0.308 ± 0.002)	0.0066 ± 0	0.0049 ± 0.0002	0.0076 ± 0.0001

[a] Unless otherwise indicated, properties of the Lys265 mutants are reported for preparations obtained after covalent reconstitution with FAD, as described in the text. [b] Data previously reported (*5*). [c] Absorption spectra were recorded in 100 mM potassium phosphate buffer, pH 8.0, 25 °C. [d] $4xy$ = 454 (wild-type), 449 (Lys265Arg, Lys265Gln, Lys265Met) or 448 (Lys265Ala) nm. [e] Apparent turnover rates were measured at 25 °C in air-saturated 100 mM potassium phosphate buffer, pH 8.0, containing 120 mM sarcosine using a horseradish peroxidase-coupled assay, as previously described (*7*). All values are the average of two determinations. The value shown in parentheses was obtained for the isolated Lys265Arg mutant before reconstitution with FAD.

apoenzymes were reconstituted by incubation with 500 μM FAD for 3.5 h in 50 mM Tris buffer, pH 8.0, at room temperature. The reconstituted samples were subjected to ultrafiltration (CentriPrep YM30 column) to remove unbound FAD and change the buffer to 100 mM potassium phosphate, pH 8.0. The concentration of wild-type MSOX and the reconstituted mutant enzymes was estimated on the basis of flavin absorbance by using the extinction coefficients listed in Table 2. Catalytic activity was monitored by using a horseradish peroxidase-coupled assay with *o*-dianisidine as the chromogenic substrate (*7*).

Steady-State Spectroscopy and Flavin Analysis. Absorption spectra were recorded using an Agilent Technologies 8453 diode array or a Perkin-Elmer Lambda 25 spectrophotometer. Extinction coefficients and the stoichiometry of FAD incorporation into the isolated and/or reconstituted Lys265 mutant preparations were determined after denaturation of the mutant enzyme preparations with guanidine hydrochloride, as previously described (*5*). Dissociation constants for the complex formed with Lys265Met or Lys265Arg and methylthioacetate were determined by fitting a theoretical binding curve to absorbance changes observed at 515 or 518 nm, respectively. Spectra corresponding to 100% complex formation were calculated as previously described (*12*). Special cuvettes with two sidearms were used for anaerobic experiments. The cuvettes were made anaerobic by bubbling argon through protein-free solutions in the main compartment or over the surface of small aliquots of enzymes in the sidearms.

Kinetics of the Anaerobic Reduction of Lys265Met, Lys265Arg or Wild-Type MSOX with Sarcosine. The anaerobic reductive half-reactions were monitored using a Hi-Tech Scientific SF-62DX2 stopped-flow spectrometer with diode array detection. All spectra are averages of at least five replicate shots, collected in log mode to maximize the number of points acquired during the early phase of each reaction. Solutions containing enzyme or sarcosine were prepared in buffer containing 50 mM glucose. The solutions were made anaerobic by multiple cycles of evacuation, followed by flushing with oxygen-scrubbed argon. Glucose oxidase was then tipped from a sidearm of the tonometer to a final concentration of 14.7 units/mL to remove traces of residual oxygen. The entire flow circuit of the stopped-flow spectrometer was made anaerobic by an overnight incubation with anaerobic buffer containing 50 mM glucose and glucose oxidase (14.7 unit/mL).

Global analyses of absorption spectra acquired for the reductive half-reactions were performed using Specfit 3.0, a software package that generates calculated spectra of intermediates, rate constants for intermediate formation and decay, and yields of the intermediate(s) as a function of reaction time. The enzyme·substrate charge transfer complex formed with Lys265Met or Lys265Arg was characterized using initial spectra recorded after mixing the mutant enzymes with a range of different sarcosine concentrations. Dissociation constants for the complexes were determined by fitting a theoretical binding curve to initial absorbance changes observed at 495 or 497 nm, respectively. Spectra corresponding to 100% complex formation were calculated as previously described (*12*). Fitting of single-wavelength kinetics traces were conducted using Sigma Plot 10 (Systat Software).

Kinetics of the Reaction of Reduced Lys265Met with Molecular Oxygen. A concentrated stock solution of reduced Lys265Met (75 μM) in 100 mM potassium phosphate buffer, pH 8.0, at 25 °C was prepared by reaction with 1 equiv of sarcosine in an anaerobic cuvette. The reduced enzyme was diluted at least 10-fold by injecting an aliquot of the stock solution into a special screw-cap cuvette equipped with a Teflon-silicon membrane (Spectrocell) using a gastight Hamiliton syringe that had been flushed with oxygen-scrubbed argon gas. The sealed screw-cap cuvettes contained 100 mM potassium phosphate buffer, pH 8.0, at 25 °C that

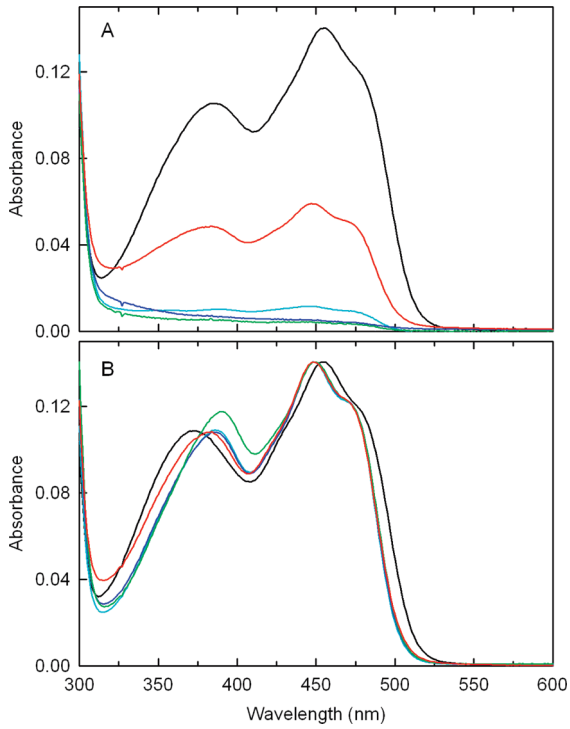

FIGURE 2: Comparison of the spectral properties of wild-type MSOX with that observed with Lys265 mutants before (panel A) and after (panel B) reconstitution of the mutant preparations with FAD. Absorption spectra of wild-type MSOX, Lys265Arg, Lys265Ala, Lys265Met, and Lys265Gln are shown in the black, red, cyan, blue, and green curves, respectively. All spectra were recorded at 25 °C in 100 mM potassium phosphate buffer, pH 8.0. Spectra in panel A are normalized to that same absorbance at 280 nm. Spectra in panel B are normalized to the same absorbance at the lower energy absorption maximum (λ_{max} = 454 (wild-type), 449 (Lys265Arg, Lys265Gln, Lys265Met) or 448 (Lys265Ala) nm.

had been equilibrated with water-saturated gas mixtures containing 9.98, 21.05, 44.00 or 100% oxygen (balance nitrogen). The reactions were monitored using an Agilent Technologies 8453 diode array spectrophotometer.

Kinetics of the Reaction of Reduced Lys265 Arg or Wild-Type MSOX with Molecular Oxygen. A 15 μM solution of reduced Lys265Arg or wild-type MSOX was prepared in a stopped-flow tonometer. The main compartment of the tonometer was filled with 100 mM potassium phosphate buffer, pH 8.0, containing 1 equiv of sarcosine; a small aliquot of concentrated enzyme was placed in the sidearm of the tonometer. The solutions were made anaerobic by multiple cycles of evacuation, followed by flushing with oxygen-scrubbed argon. Since the glucose/glucose oxidase system could not be used in these experiments, an additional step was included to remove traces of oxygen. In this approach, oxygen-scrubbed argon gas was bubbled directly through the buffer in the main compartment and over the surface of the enzyme in the sidearm of the tonometer. The aliquot of Lys265Arg or wild-type MSOX was then reduced by tipping the contents of the sidearm into the main compartment of the tonometer. Reduction of wild-type enzyme was complete upon mixing. The Lys265Arg sample was incubated for 30 min at room temperature to ensure complete reaction. The reaction of reduced Lys265Arg or wild-type MSOX with oxygen at 25 °C was monitored by following the increase in absorption at 449 or 454 nm, respectively, using a Hi-Tech Scientific SF-62DX2 stopped-flow spectrometer in photomultiplier mode. In these experiments, reduced enzyme was mixed (1:1) with 100 mM potassium phosphate buffer, pH 8.0, that had been equilibrated with water-saturated gas mixtures containing 21.05, 44.00, 64.97 or 100% oxygen (balance nitrogen).

RESULTS

Effect of Lys265 Mutations on Holoenzyme Biosynthesis. Conservative mutation of Lys265 to Arg results in the isolation of a preparation that contains covalently bound FAD and exhibits a typical flavoprotein spectrum (Figure 2A, red curve). However, the covalent flavin content of the isolated mutant preparation (0.25 mol of FAD/mol of protein) is less than 30% of that observed with wild-type MSOX (Table 2). A more dramatic effect on *in vivo* flavinylation is observed upon replacing Lys265 with neutral residues. The isolated preparation of Lys265Ala exhibits a recognizable flavin absorption spectrum (Figure 2A, cyan curve) but contains only 0.05 mol of FAD/mol of protein. The isolated preparations of Lys265Met and Lys265Gln contain no detectable FAD and exhibit low intensity, characterless absorption in the visible region (Figure 2A, blue and green curves, respectively).

Reconstitution of the Lys265 Mutant Apoproteins with FAD. The isolated Lys265 mutant preparations were incubated for 3.5 h with 500 μM FAD and then treated to remove free FAD, as detailed in Experimental Procedures. Remarkably, all of the mutant enzymes incorporated substantial amounts of flavin that was covalently attached to the protein, as judged by ultrafiltration of the reconstituted enzymes after denaturation with 3.0 M guanidine hydrochloride. The reconstituted mutant preparations exhibit 62 to 85% of the covalent flavin content observed with wild-type MSOX (Table 2). The results show that the isolated Lys265 mutant apoproteins retain the ability to catalyze covalent flavin biosynthesis.

Spectral and Catalytic Properties of the Reconstituted Lys265 Mutant Enzymes. All of the reconstituted Lys265 mutant enzymes exhibit typical flavoprotein absorption spectra with two maxima in the visible region (Figure 2B). The higher energy absorption band exhibits a somewhat more pronounced shoulder and is hypsochromically shifted (6−7 nm) in the mutant enzymes compared with the 454 nm absorption band observed with wild-type MSOX. The lower energy absorption band in the mutant enzymes is bathochromically shifted (11−17 nm) compared with wild-type MSOX (Table 2). The mutations do not affect relative intensity of the two absorption bands, except for Lys265Gln where the intensity of the lower energy band is somewhat enhanced compared with wild-type MSOX.

In contrast to the relatively modest spectral perturbations, mutation of Lys265 to a neutral residue results in an enormous decrease in catalytic activity, as judged by apparent turnover rates observed in air-saturated buffer containing 120 mM sarcosine. A 6000- to 9000-fold decrease in the apparent turnover rate is observed when Lys265 is changed to Ala, Gln, or Met. A substantial decrease in apparent turnover rate (170-fold) is observed even when Lys265 is conservatively replaced by arginine (Table 2). To elucidate the apparently critical role of Lys265 in catalysis, the Lys265Met and Lys265Arg mutants were selected for detailed studies.

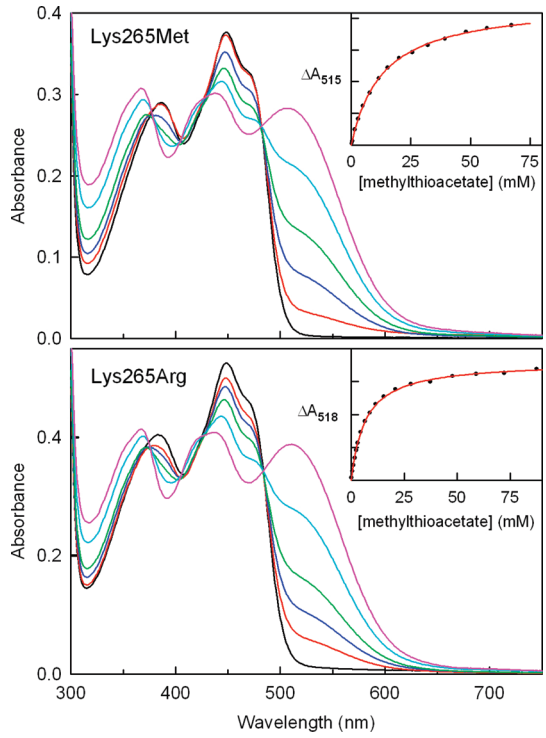

FIGURE 3: Spectral titration of Lys265Met (A, top panel) or Lys265Arg (B, bottom panel) with methylthioacetate. Titrations were conducted at 25 °C in 100 mM potassium phosphate buffer, pH 8.0. The black curve in each panel was recorded for the ligand-free enzyme. The magenta curve in each panel is the spectrum calculated for 100% complex formation, as described in Experimental Procedures. A, top panel: The red, blue, green and cyan curves were recorded after addition of 1.48, 4.88, 11.6 and 39.3 mM methythioacetate, respectively. B, bottom panel: The red, blue, green and cyan curves were recorded after addition of 1.09, 2.34, 4.53 and 15.3 mM methythioacetate, respectively. The insets in the top and bottom panels show plots of the observed absorbance increases at 515 and 518 nm, respectively. The solid red lines were obtained by fitting a theoretical binding curve ($\Delta A_{obs} = \Delta A_{max}[ligand]/(K_d + [ligand])$ to the data (black circles).

Does Mutation of Lys265 Affect Binding of a Competitive Inhibitor? Methylthioacetate (MTA, $CH_3SCH_2CO_2^-$) is a sarcosine analogue in which the substrate nitrogen is replaced by sulfur. The Lys265Met and Lys265Arg mutants form complexes with MTA that exhibit a new absorption band in the visible region (Figure 3), a feature diagnostic of charge transfer interaction. Wild-type MSOX also forms a charge transfer complex with MTA. However, the charge transfer bands observed with Lys265Met and Lys265Arg are shifted to shorter wavelengths (higher energy) ($\lambda_{max} = 515$ and 518 nm, respectively) compared with wild-type MSOX ($\lambda_{max} = 532$ nm), as judged by the position of the long wavelength bands in the corresponding difference spectra (see Figure 6B). Mutation of Lys265 to Met or Arg also caused a modest decrease in the stability of the MTA complex (4.6- or 2.4-fold, respectively), as judged by comparison of dissociation constants observed with mutant and wild-type MSOX (Table 3).

Does Mutation of Lys265 Affect the Kinetics of Enzyme Reduction by Sarcosine? The observed shift of the MTA charge transfer band to higher energy suggested that mutation of Lys265 might lower the flavin reduction potential, similar to that observed with the Arg49Lys mutant (*30*). A lower flavin reduction potential could result in a decreased rate of sarcosine oxidation. We reasoned that the anaerobic reduction of Lys265Met with excess sarcosine would need to be extremely slow in order to account for the observed 6000-fold decrease in apparent turnover rate and should be readily monitored using a steady-state diode array spectrometer. However, a manual mixing experiment showed that reduction of Lys265Met with 120 mM sarcosine was much too fast to observe using this approach. We therefore initiated studies to characterize the kinetics of the anaerobic reaction of Lys265Met or Lys265Arg with sarcosine using a stopped-flow diode array spectrometer, as detailed in the following sections.

Characterization of an Enzyme·Substrate Complex Formed with Lys265Met or Lys265Arg. The initial spectrum observed after mixing Lys265Met with 140 mM sarcosine (Figure 4A, curve 1) differs from that obtained in the absence of sarcosine (Figure 4A, red curve), especially with respect to the development of absorbance in the long-wavelength region ($\lambda > 480$ nm). This feature suggested that the reductive half-reaction with Lys265Met is initiated by the formation of an enzyme·substrate charge transfer complex, similar to that observed with wild-type MSOX (*12*). Consistent with this hypothesis, initial spectra observed after mixing Lys265Met with a wide range of sarcosine concentrations (1 to 140 mM) are isosbestic (Figure 5A) and show the progressive formation of a charge transfer band that exhibits a maximum at 495 nm, as estimated by the position of the peak in the corresponding difference spectrum (Figure 6A). The observed maximum is shifted to shorter wavelengths compared with that seen with wild-type MSOX ($\lambda_{max} = 516$ nm), similar to results obtained for the MTA complexes. Sarcosine also forms a charge transfer complex with the Lys265Arg mutant (Figure 5B). The spectral properties of the Lys265Arg·sarcosine charge transfer complex ($\lambda_{max} = 497$ nm) more closely resemble those observed with Lys265Met than wild-type MSOX, as judged by comparison of the corresponding difference spectra where a positive band at 408 nm is seen with wild-type MSOX but not with the mutant enzymes (Figure 6A). Dissociation constants determined for the sarcosine complexes with Lys265Met or Lys265Arg (see insets in Figure 5) indicate that the mutant complexes are somewhat less stable than the corresponding wild-type complex, similar to that observed with the MTA complexes (Table 3).

Detection of a Novel Intermediate during Reduction of Lys265Met or Lys265Arg with Sarcosine. An isosbestic spectral course is observed for the anaerobic reduction of wild-type MSOX over a wide range of sarcosine concentrations (1 to 80 mM) in reactions that exhibit a monophasic exponential loss of oxidized enzyme absorbance (*12*). Apparently similar features are observed for the reductive half-reactions with Lys265Met or Lys265Arg but only at sarcosine concentrations below 25 or 10 mM, respectively (data not shown, see Supporting Information Figure S1). Reactions observed with the Lys265 mutants at higher sarcosine concentrations are not isosbestic and exhibit a biphasic loss of oxidized flavin absorbance (Figures 4A and 7A). However, it is noteworthy that the same final reduced enzyme spectrum is observed with the Lys265 mutants over the entire range of sarcosine concentrations tested in these studies (1 to 140 mM). Importantly, the final spectra of the reduced mutant enzymes closely resemble that observed in

Table 3: Properties of Charge Transfer Complexes Formed with Methylthioacetate or Sarcosine and Wild-Type MSOX or Lys265 Mutants[a]

	methylthioacetate complex			sarcosine complex		
preparation	K_d (mM)	λ_{max} (nm)	$\Delta\epsilon_{\lambda_{max}}$ (M^{-1} cm^{-1})	K_d (mM)	λ_{max} (nm)	$\Delta\epsilon_{\lambda_{max}}$ (M^{-1} cm^{-1})
wild-type[b]	2.88 ± 0.04	532	7710	13.0 ± 0.1	516	3870
Lys265Met	13.3 ± 0.3	515	9690	58 ± 10	495	3600
Lys265Arg	6.9 ± 0.1	518	8980	34 ± 1	497	3860

[a] All measurements were made in 100 mM potassium phosphate buffer, pH 8.0 at 25 °C. The λ_{max} for each charge transfer complex was determined on the basis of maxima observed in difference spectra, as described in the text. Dissociation constants were determined by fitting a theoretical binding curve to the observed development of the charge transfer absorption band as a function of ligand concentration, as detailed in the legends to Figures 3 and 5. [b] Data for the wild-type enzyme complexes with methylthioacetate and sarcosine were taken from Zhao et al. (*42*) and Zhao and Jorns (*12*), respectively

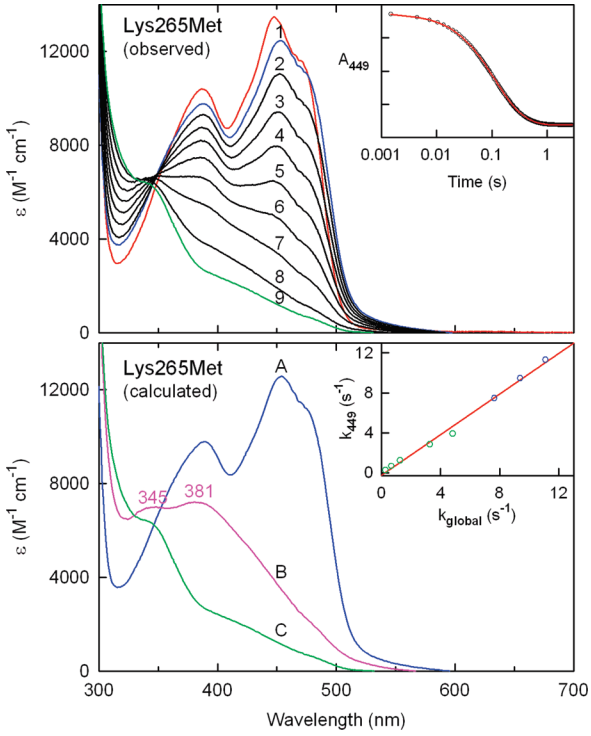

FIGURE 4: Anaerobic reaction of Lys265Met with sarcosine monitored by stopped-flow diode array spectroscopy. A, top panel: Curves 1 to 9 were obtained from 1.49 ms to 1.65 s after mixing the enzyme with 140 mM sarcosine in 100 mM potassium phosphate buffer, pH 8.0, containing 50 mM glucose and glucose oxidase (14.7 units/mL) at 25 °C. The red curve is absorption spectrum of substrate-free enzyme obtained under otherwise identical conditions. The inset shows a plot of the observed absorbance decrease at 449 nm. The red line was obtained by fitting a double exponential equation ($y = Ae^{-k_1t} + Be^{-k_2t} + C$) to the data (open circles). B, bottom panel: Calculated spectra obtained by global fitting of a model, A → B → C, to the observed diode array data, as detailed in the text. The inset shows a plot of rate constants calculated for the conversion of A to B by global analysis versus values obtained by analysis of reaction traces at 449 nm. The green and blue circles correspond to results obtained for reactions at "lower" and "higher" sarcosine concentrations, as detailed in the text. The red line was obtained by linear regression analysis of the entire data set ($r^2 = 0.9931$, slope = 1.02 ± 0.03).

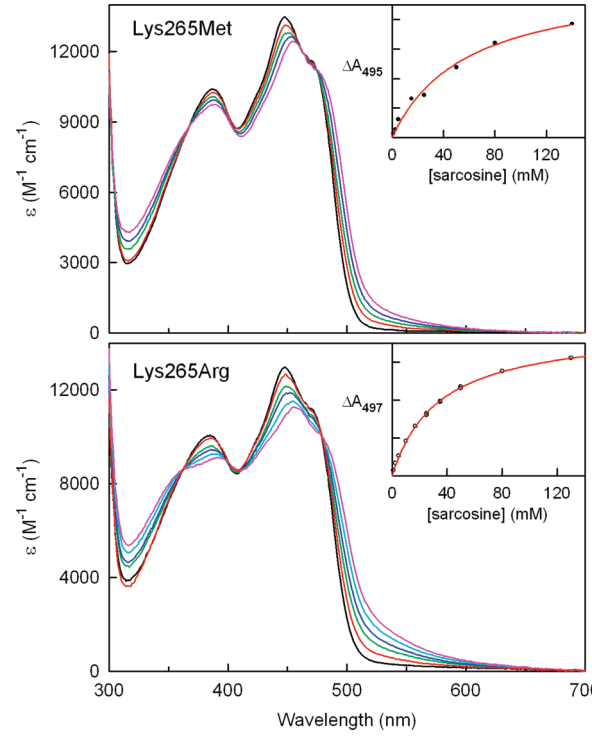

FIGURE 5: Formation of a charge transfer complex as detected upon mixing Lys265Met (A, top panel) or Lys265Arg (B, bottom panel) with various concentrations of sarcosine in a stopped-flow diode array spectrometer. Spectra were recorded in anaerobic buffer, as detailed in the legends to Figures 4 and 7. The black curve in each panel was obtained for substrate-free enzyme. The magenta curve in each panel is the spectrum calculated for 100% sarcosine complex formation, as described in Experimental Procedures. A, top panel: Initial spectra (time indicated in parentheses) recorded after mixing Lys265Met with 15, 50 and 140 mM sarcosine are shown in the red (3.74 ms), green (3.74 ms) and blue (1.49 ms) curves, respectively. B, bottom panel: Initial spectra (time indicated in parentheses) recorded after mixing Lys265Arg with 10, 25, 50 and 130 mM sarcosine are shown in the red (3.74 ms), green (0.74 ms), blue (0.74 ms), and cyan (0.74 ms) curves, respectively. The insets in the top and bottom panels show plots of observed absorption increases at 495 and 497 nm, respectively. The solid red lines were obtained by fitting a theoretical binding curve ($\Delta A_{obs} = \Delta A_{max}[ligand]/(K_d + [ligand])$ to the data (black circles).

the monophasic reductive half-reactions seen with wild-type MSOX (*12*).

The results strongly suggested that a novel spectral intermediate is formed during reduction of the Lys265 mutants, at least at "higher" sarcosine concentrations. To evaluate this hypothesis, a global analysis was performed by fitting a model, A → B → C, to spectra obtained for the reductive half-reactions observed with Lys265Met or Lys265Arg at sarcosine concentrations above 25 or 10 mM, respectively. Species A in this model corresponds to the initial equilibrium mixture of free enzyme and the enzyme•sarcosine charge transfer complex which is formed within the instrument dead time, B is the postulated intermediate and C is the final reduced enzyme species. A good fit of the proposed model was obtained, as illustrated by results obtained for the reaction of Lys265Met with 140 mM sarcosine (Figure 4B) or Lys265Arg with 130 mM sarcosine (Figure 7B). As predicted, calculated absorption spectra of species A and C superimpose with initial and final observed spectra, respectively. The calculated spectrum of species A

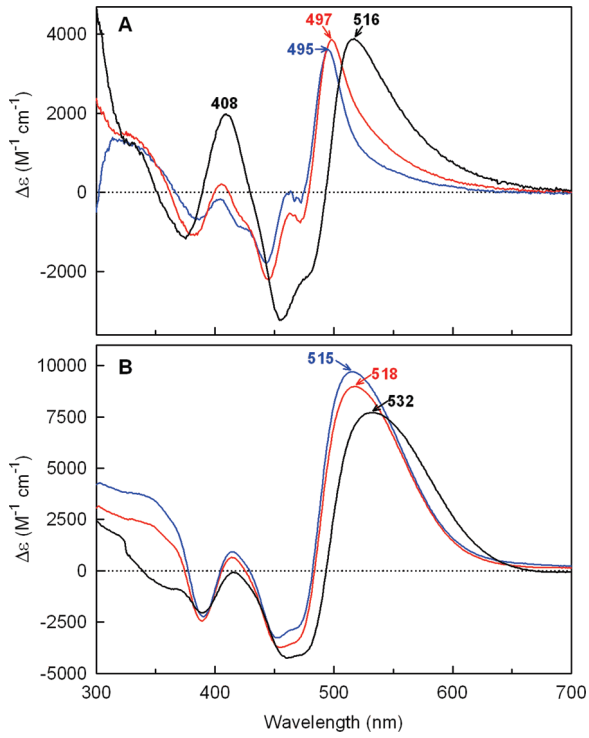

FIGURE 6: Comparison of difference spectra calculated for 100% charge transfer complex formation with sarcosine (panel A) or methylthioacetate (panel B). The blue, red and black curves in each panel are difference spectra calculated for 100% complex formation with Lys265Met, Lys265Arg and wild-type MSOX, respectively. The data for the wild-type complexes with methylthioacetate and sarcosine were taken from Zhao et al. (*42*) and Zhao and Jorns (*12*), respectively.

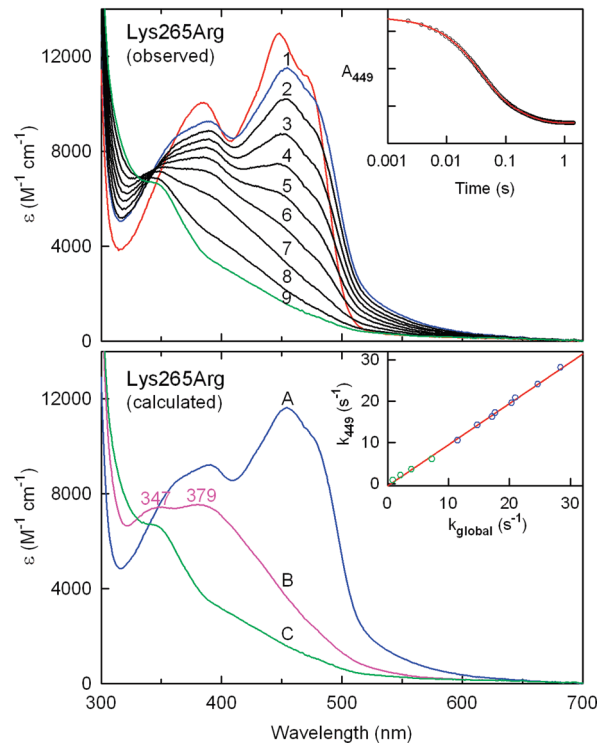

FIGURE 7: Anaerobic reaction of Lys265Arg with sarcosine monitored by stopped-flow diode array spectroscopy. A, top panel: Curves 1 to 9 were obtained from 0.74 ms to 1.425 s after mixing the enzyme with 130 mM sarcosine in 100 mM potassium phosphate buffer, pH 8.0, containing 50 mM glucose and glucose oxidase (14.7 units/mL) at 25 °C. The red curve is the absorption spectrum of substrate-free enzyme obtained under otherwise identical conditions. The inset shows a plot of the observed absorbance decrease at 449 nm. The red line was obtained by fitting a double exponential equation ($y = Ae^{-k_1t} + Be^{-k_2t} + C$) to the data (open circles). B, bottom panel: Calculated spectra obtained by global fitting of a model, A → B → C, to the observed diode array data, as detailed in the text. The inset shows a plot of rate constants calculated for the conversion of A to B by global analysis versus values obtained by analysis of reaction traces at 449 nm. The green and blue circles correspond to results obtained for reactions at "lower" and "higher" sarcosine concentrations, as detailed in the text. The red line was obtained by linear regression analysis of the entire data set ($r^2 = 0.9982$, slope = 0.99 ± 0.01).

varied depending on the substrate concentration whereas the same calculated spectrum was obtained for intermediate B or species C independent of the sarcosine concentration. Very similar calculated spectra for intermediate B are obtained upon analysis of the reactions observed with Lys265Met (λ_{max} = 345, 381 nm) or Lys265Arg (λ_{max} = 347, 379 nm). Values obtained by global analysis for the rate of intermediate B formation (k_1) or the rate of intermediate B conversion to species C (k_2) are in excellent agreement with results obtained by fitting a double exponential equation to the corresponding reaction traces observed at 449 nm (see insets in Figures 4B and 7B). For each mutant, the observed rate of intermediate B formation varied depending on the sarcosine concentration whereas the observed rate of intermediate B conversion to species C was independent of the substrate concentration. Importantly, the calculated maximal yield of intermediate B was positively correlated with the sarcosine concentration over the range of "higher" substrate concentrations included in these analyses. This outcome suggested that intermediate B is also formed at lower sarcosine concentrations, albeit at slower rates that would reduce the maximal yield of the intermediate and its made detection more difficult.

To evaluate this hypothesis, global analyses were performed using the calculated spectrum of intermediate B in fitting a model, A → B → C, to spectra obtained for the reductive half-reactions at the lower range of sarcosine concentrations. In each case, spectra calculated for species A and C coincided with observed initial and final spectra, respectively. Significantly, values obtained for k_2 were independent of the substrate concentration and similar to those obtained for the reactions at "higher" sarcosine concentrations. Most importantly, values calculated for k_1 by global analysis of the reactions at the lower range of sarcosine concentrations varied depending on the substrate concentration and were in good agreement with rate constants estimated by fitting a single exponential equation to the corresponding reaction traces observed at 449 nm (see insets in Figures 4B and 7B).

Does Intermediate B Contain Reduced Flavin? The calculated absorption spectrum suggested that flavin reduction occurs during formation of intermediate B. In this case, the observed rate of intermediate B formation should exhibit a substantial kinetic isotope effect (KIE) whereas the rate of intermediate B conversion to species C should be unaffected when the methyl group protons in sarcosine are replaced by deuterium. Intriguingly, this scenario suggested that the reductive half-reaction with a high concentration of deuterated substrate might resemble that observed for the reaction with a low concentration of unlabeled sarcosine. Consistent with this hypothesis, the anaerobic half-reaction of Lys265Met with 140 mM [N-methyl-D_3]-sarcosine ex-

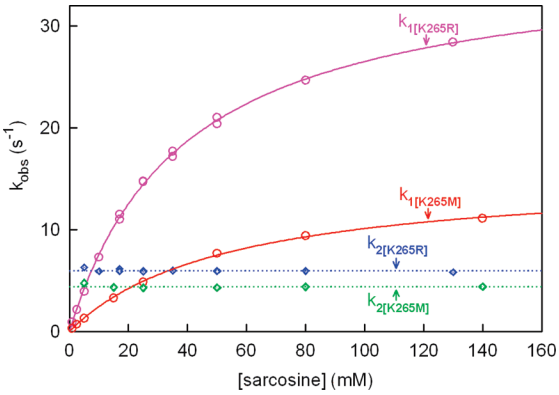

FIGURE 8: Effect of sarcosine concentration on the observed rate of formation of intermediate B (k_1) and species C (k_2) during the anaerobic reduction of Lys265Met or Lys265Arg as monitored by stopped-flow diode array spectroscopy. Values for k_1 and k_2 were determined by global fitting of a model, A → B → C, to spectra observed for reactions at each sarcosine concentration, as detailed in the text. Values obtained for k_1 with Lys265Met and Lys265Arg are shown by the red and magenta open circles, respectively. The corresponding solid red and magenta lines were obtained by fitting a hyperbolic equation ($k_{1_{obs}} = k_{lim}$[sarcosine]/($K_{d_{app}}$ + [sarcosine])) to the data. Values obtained for k_2 with Lys265Met and Lys265Arg are shown by the green and blue open diamonds, respectively. (For clarity, two points at [sarcosine] ≤ 2.5 mM are not shown.) The dotted green and blue lines correspond to the average value obtained for k_2 with Lys265Met and Lys265Arg, respectively.

Table 4: Kinetic Parameters for the Reductive Half-Reaction of Wild-Type MSOX or Lys265 Mutants with Sarcosine[a]

preparation	k_{lim} (s^{-1})	$K_{d_{app}}$ (mM)	k_2 (s^{-1})
wild-type[b]	140 ± 3	13.9 ± 0.7	nd
Lys265Met[c]	15.5 ± 0.3	54 ± 2	4.8 ± 0.3
Lys265Arg[c]	36.8 ± 0.5	39 ± 1	6.06 ± 0.07

[a] All kinetic parameters were determined in 100 mM potassium phosphate buffer, pH 8.0, at 25 °C. [b] The kinetic paramenters for the reduction of wild-type MSOX were previously reported (*12*). A second phase is not detected in these reactions which exhibit monoexponential kinetics. [c] Biexponential kinetics are observed for the reduction of the Lys265 mutants. Rate constants observed for the first phase of the reaction exhibit a hyperbolic dependence on sarcosine concentration, as discussed in the text; k_{lim} is the limiting rate of this phase at saturating sarcosine. The second phase (k_2) is independent of the sarcosine concentration.

hibits an isosbestic spectral course and a monophasic exponential loss of oxidized enzyme absorbance (data not shown; see Supporting Information Figure S2), as observed for the reaction with a 1.0 mM unlabeled sarcosine (see Figure S1) but unlike results obtained with 140 mM unlabeled substrate (see Figure 4A). A global analysis of the reductive half-reaction with 140 mM deuterium-labeled sarcosine was performed using the calculated spectrum of intermediate B in fitting a model, A → B → C, to the data. As predicted, fairly similar values are obtained for the rate of intermediate B conversion to species C with labeled (k_2^D = 6.6 ± 0.1 s^{-1}) or unlabeled (k_2^H = 4.41 ± 0.02 s^{-1}) sarcosine. In contrast, the observed rate of intermediate B formation with deuterated sarcosine (k_1^D = 1.260 ± 0.002 s^{-1})[2] is nearly 9-fold slower (KIE = k_1^H/k_1^D = 8.77 ± 0.05) than observed with unlabeled sarcosine (k_1^H = 11.05 ± 0.06 s^{-1}). A substantial kinetic isotope effect is also observed for

[2] The value obtained for k_1^D by global analysis is similar to a value obtained by fitting a single exponential equation to the reaction trace observed at 449 nm (k^D = 1.218 ± 0.002 s^{-1}).

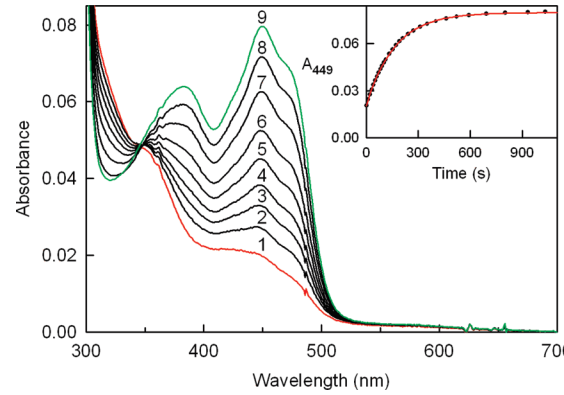

FIGURE 9: Oxidation of reduced Lys265Met (5.9 μM) by reaction with molecular oxygen (117 μM) as monitored by steady-state diode array spectroscopy in 100 mM potassium phosphate buffer, pH 8.0 at 25 °C. A concentrated anaerobic stock solution of the mutant enzyme (75 μM) was reduced by reaction with a stoichiometric amount of sarcosine and then diluted into buffer that had been equilibrated with a water-saturated gas mixture containing 9.98% oxygen (balance nitrogen), as detailed in Experimental Procedures. Curves 1 to 9 were recorded at 1.4, 22, 42, 62, 92, 132, 212, 352 and 1032 s after dilution, respectively. The inset shows a plot of the observed absorption increase at 449 nm. The red line was obtained by fitting an equation for a single exponential rise [$y = A(1 - e^{-kt}) + B$] to the data (black circles).

reduction of wild-type MSOX with sarcosine (KIE = 5.93 ± 0.03), as judged by results obtained with 140 mM unlabeled (k^H = 119.6 ± 0.4 s^{-1}) versus deuterium-labeled (k^D = 20.16 ± 0.06 s^{-1}) substrate.

Effect of Substrate Concentration on the Kinetics of Formation and Decay of Intermediate B. The observed rate of intermediate B formation (k_1) exhibits a hyperbolic dependence on sarcosine concentration, as judged by values obtained by global analysis of the reductive half-reactions observed with Lys265Met or Lys265Arg over the entire range of substrate concentrations (Figure 8). The corresponding double-reciprocal plots are linear with a finite *Y*-intercept (plot not shown). Values for the limiting rate of formation of intermediate B at saturating sarcosine (k_{lim}) and the apparent dissociation constant for the enzyme·substrate charge transfer complex ($K_{d_{app}}$) were estimated by fitting eq 1 to the data (Table 4). Values obtained for $K_{d_{app}}$ by kinetic analysis are in good agreement with K_d values determined on the basis of the observed spectral properties of the enzyme·substrate complexes (Table 3). This outcome is expected for a nonsticky substrate where the rate of complex dissociation is much faster than its conversion to intermediate B.

$$k_{1obs} = k_{lim}[\text{sarcosine}]/(K_{d_{app}} + [\text{sarcosine}]) \quad (1)$$

Unlike intermediate B formation, the observed rate of intermediate B conversion to species C (k_2) is independent of the sarcosine concentration (see Figure 8 and Table 4). Overall, despite a large difference in apparent turnover rates, values obtained for the three parameters that define the kinetics of the reductive half-reactions with the two Lys265 mutants ($K_{d_{app}}$, k_{lim}, and k_2) are remarkably similar, exhibiting a maximal difference of less than 2.5-fold (Table 4).

Inspection of the plots in Figure 8 shows that the overall rate of the reductive half-reaction with either mutant at *saturating concentrations of sarcosine* will be limited by the rate of conversion of intermediate B to the final reduced

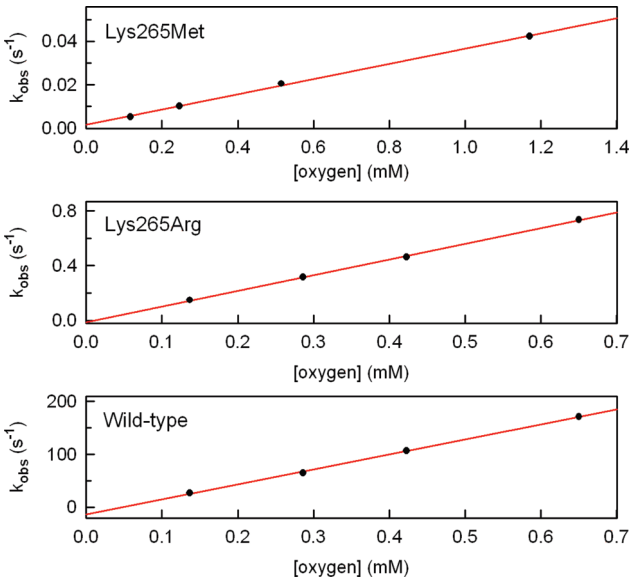

FIGURE 10: Effect of oxygen concentration on the observed rate of reoxidation of reduced Lys265Met (A, top panel), Lys265Arg (B, middle panel) or wild-type MSOX (C, bottom panel). The reaction of reduced Lys265Met was monitored by steady-state diode array spectroscopy, as described in the legend to Figure 9. The reaction of reduced Lys265Arg or wild-type MSOX was monitored at 449 or 454 nm, respectively, using a stopped-flow spectrometer in photomultiplier mode. Values for k_{obs} with mutant or wild-type enzyme were obtained by fitting an equation for a single exponential rise to observed changes in absorption at 449 or 454 nm, respectively. The red lines were generated by linear regression analysis of data obtained with Lys265Met, Lys265Arg and wild-type MSOX ($r^2 = 0.9987$, 0.9993, and 0.9989, respectively).

Table 5: Rate Constants for the Oxidation of Reduced Wild-Type MSOX or Lys265 Mutants by Molecular Oxygen

preparation	k_{obs} (M^{-1} s^{-1})	$k_{predicted}$ (M^{-1} s^{-1})[a]
wild-type	$2.83 \pm 0.07 \times 10^5$	$1.68 \pm 0.02 \times 10^5$
Lys265Met	35.1 ± 0.9	27.8 ± 0.4
Lys265Arg	1140 ± 20	996 ± 4
free flavin[b]	250	

[a] The predicted values were calculated using values obtained for $k_{cat_{app}}$ (see Table 2) and the assumption that oxidation of the reduced enzymes was fully rate-determining during turnover in air-saturated buffer (273 μM oxygen). [b] Data previously reported (*1*).

enzyme species (k_2). Values obtained for k_2 with the Lys265 mutants are about 25-fold slower than the limiting rate of the reductive half-reaction observed with wild-type MSOX (Table 4). Importantly, the results show that the 170- or 6000-fold decrease in apparent turnover rates observed with Lys265Arg or Lys265Met, respectively, cannot be explained by the relatively modest effects of these mutations on the rate of the reductive half-reaction.

Reaction of Reduced Lys265Met, Wild-Type MSOX or Lys265Arg with Oxygen. The reductive half-reaction studies suggested that product release or an extremely slow reaction of reduced Lys265Met with oxygen might account for the 6000-fold decrease in the apparent turnover rate observed with this mutant. To test the oxygen reactivity hypothesis, a stock solution of reduced Lys265Met was prepared by anaerobic reaction of the enzyme with 1 equiv of sarcosine. An aliquot of reduced enzyme was then injected into a sealed cuvette containing buffer that had been equilibrated with water-saturated gas mixtures containing 9.98 to 100% oxygen (balance nitrogen). Indeed, the kinetics of oxidation of reduced Lys265Met were quite slow over the entire range of oxygen concentrations and could be monitored using a steady-state diode array spectrometer. In each case, a virtually isosbestic conversion of reduced to oxidized enzyme was observed in reactions that exhibit a monophasic exponential increase in absorbance at 449 nm, as illustrated by results obtained for the reaction with 117 μM oxygen (Figure 9). Rate constants observed at different concentrations of oxygen were directly proportional to oxygen concentration (Figure 10A). The second-order rate constant for the oxidation of reduced Lys265Met was determined from the slope of this plot. Remarkably, the value obtained with reduced Lys265Met ($k = 35.1 \pm 0.9$ M^{-1} s^{-1}) is actually 7-fold slower than the sluggish reaction observed with free reduced flavin (Table 5).

The kinetics of the much faster oxidative half-reaction with wild-type MSOX could be observed using a stopped-flow spectrometer in photomultiplier mode. In these experiments, a 15 μM solution of substrate-reduced wild-type MSOX was mixed (1:1) with buffer that had been equilibrated with water-saturated gas mixtures containing 21.05 to 100% oxygen (balance nitrogen). The reaction was monitored by following the increase in absorption due to the oxidized enzyme at 454 nm. Rate constants determined for the monophasic reactions are directly proportional to the oxygen concentration (Figure 10C). Oxidation of reduced wild-type MSOX is a very rapid bimolecular reaction ($k = 2.83 \pm 0.07 \times 10^5$ M^{-1} s^{-1}) that is more than 1000-fold faster that the reaction observed with free reduced flavin. The results obtained with wild-type MSOX indicate that substitution of Lys265 with Met causes a 8000-fold decrease in the rate of the reaction of the reduced enzyme with oxygen, consistent with the observed effect of this mutation on the apparent turnover rate (Table 5).

In contrast to results obtained with reduced Lys265Met, the oxidative half-reaction with Lys265Arg was too fast to observe in a manual mixing experiment. The kinetics of the reaction with substrate-reduced Lys265Arg were determined by monitoring the increase in absorption due to the oxidized enzyme at 449 nm in a stopped-flow spectrometer, as described above in studies with wild-type enzyme. The second-order reaction of oxygen with reduced Lys265Arg (Figure 10B) ($k = 1140 \pm 20$ M^{-1} s^{-1}) is more than 30-fold faster than observed with reduced Lys265Met but 250-fold slower than observed with reduced wild-type MSOX. The results are consistent with the observed difference in the apparent turnover rates observed with these mutants (Table 5).

DISCUSSION

Mutation of Lys265 to Met, Ala, Gln or Arg results in the isolation of preparations that are largely or entirely devoid of covalently bound flavin. However, the mutant apoproteins retain the ability to catalyze covalent flavin incorporation and can be reconstituted with FAD. The basis for the adverse effect of Lys265 mutations on *in vivo* flavinylation is currently under investigation. The reconstituted Lys265 mutant preparations exhibit typical flavoprotein absorption spectra and a covalent flavin content similar (62 to 85%) to wild-type MSOX but greatly reduced catalytic activity. Mutation of Lys 265 to a neutral residue (Ala, Gln, Met) results in 6000- to 9000-fold decrease in apparent turnover

Scheme 1: Proposed Mechanism for the Reduction of Lys265 MSOX Mutants by Sarcosine[a]

$$\text{E-FAD}_{ox} + S \overset{K_d}{\rightleftharpoons} \text{E-FAD}_{ox}\bullet S$$

$$\text{E-FAD}_{ox}\bullet S \xrightarrow{k_{lim}} \text{E-FADH}_2\bullet Im$$

$$\text{E-FADH}_2\bullet Im \xrightarrow{k_2} \text{Species C}$$

[a] S = sarcosine; Im = sarcosine imine.

rate whereas a 170-fold decrease is found upon conservative replacement of Lys265 with Arg. The mutants retain the ability to bind and form charge transfer complexes with sarcosine or a competitive inhibitor (MTA), as judged by the spectral properties and stability observed for complexes formed with Lys265Met and Lys265Arg at pH 8.0. Interestingly, the zwitterionic form of sarcosine is the predominant species in solution at pH 8.0 (pK_a =10.0) whereas only the anionic form can act as a charge transfer donor. The results indicate that the pK_a of sarcosine bound to the mutant enzymes must be considerably lower than the free amino acid, similar to that observed with wild-type MSOX (*12*). Reductive half-reactions studies with Lys265Met and Lys265Arg provide evidence for a novel intermediate and show that the mutants retain the ability to oxidize sarcosine at rates that are impressively fast, especially when compared with the very slow apparent turnover rates.

A very rapid bimolecular reaction is observed with oxygen and reduced wild-type MSOX, prepared by reaction with 1 equiv of sarcosine. The results probably reflect the reactivity of the free reduced enzyme because the imine product is likely to have been lost. The rate observed in oxidative half-reaction studies with wild-type MSOX ($2.83 \pm 0.07 \times 10^5$ M^{-1} s^{-1}) is similar to a value obtained for $k_{cat}/K_{m(O_2)}$ in steady-state kinetic studies ($3.3 \pm 0.2 \times 10^5$ M^{-1} s^{-1}) (*7*) and close to the fastest rate reported for the reaction of oxygen with a reduced flavoprotein oxidase (1×10^6 M^{-1} s^{-1}) (*31*). The steady-state kinetic parameter provides an approximate estimate of the rate of reaction of oxygen with a reduced MSOX·imine product complex, the species that reacts with oxygen during turnover (*7*). Comparison of rate constants obtained with wild-type enzyme and the Lys265 mutants shows that substitution of Lys265 with a neutral residue causes a dramatic 8000-fold decrease in the rate of reaction of the reduced enzyme with oxygen and that a substantial decrease (250-fold) occurs even upon conservative replacement of Lys265 with Arg. The results provide definitive evidence for Lys265 as the site of oxygen activation in MSOX. Multiple sequence alignments and structural data indicate that Lys265 is conserved in *N*-methyltryptophan oxidase (*23*) and pipecolate oxidase (*24*) and either conserved or conservatively replaced by a histidine in fructosyl amino acid oxidase, depending on the organism (*17, 18*).

The nature of the novel intermediate observed during reduction of Lys265 mutants and the possible mechanism of oxygen activation by Lys265 are discussed in the following sections.

Effect of Lys265 Mutations on the Reductive Half-Reaction. The kinetics observed for the reduction of the Lys265Met or Lys265Arg with sarcosine are consistent with a mechanism involving a rapidly attained equilibrium between the free enzyme and the enzyme·substrate charge transfer complex, followed by an essentially irreversible conversion (k_{lim}) of the enzyme·substrate complex to an intermediate (B) that undergoes an apparent first-order conversion (k_2) to a final reduced enzyme species (C). The kinetic isotope effect observed when the methyl group protons in sarcosine are replaced by deuterium indicates that substrate oxidation occurs during conversion of the enzyme·sarcosine charge transfer complex to intermediate B (KIE = 8.77 ± 0.05). The results strongly suggest that intermediate B is a reduced enzyme·imine product complex (Scheme 1). A spectrally similar intermediate, detected during substrate reduction of wild-type dimethylglycine oxidase (DMGO), has also been attributed to a reduced enzyme·imine product complex (*32*). Intermediate B is most readily detected during reaction of the Lys265 mutant enzymes with "higher" concentrations of unlabeled sarcosine where formation of intermediate B is relatively rapid compared with its conversion to species C. A spectral intermediate is not detected during reduction of wild-type MSOX. However, it is important to note that the absorption spectrum of substrate-reduced wild-type enzyme (*12*) is virtually identical to species C observed with the Lys265 mutants. The results strongly suggest that intermediate B is also formed during reduction of wild-type MSOX but is not detectable owing to a very rapid conversion of the intermediate to species C. The limiting rate of intermediate B formation with Lys265Met or Lys265Arg at saturating sarcosine (k_{lim}) is 9.0- or 3.8-fold slower, respectively, than the limiting rate of reduction of wild-type MSOX (Table 4). The results indicate that the Lys265 mutations cause only a very modest decrease in the actual rate of sarcosine oxidation.

The overall rate of the reductive half-reactions observed with the Lys265 mutants at saturating sarcosine is, however, about 25-fold slower than observed with wild-type MSOX because the mutant reactions are limited by the rate of conversion of intermediate B to species C (k_2). The most obvious explanation is that this conversion involves release of the imine product, as proposed by Scrutton et al. for the corresponding step in the DMGO reaction (*32*). However, species C in the MSOX reactions cannot be free reduced enzyme because it formed at a catalytically significant rate during reduction of wild-type MSOX with sarcosine (*12*) and steady-state kinetic studies with the wild-type enzyme indicate that a reduced enzyme·imine complex is the species that reacts with oxygen (*7*). An alternate explanation is suggested by the fact that the spectral properties of reduced flavins are highly sensitive to changes in the local environment (*33*). This feature suggests that conversion of intermediate B to species C might simply involve isomerization of an initial reduced enzyme·imine complex to a more stable complex. A somewhat analogous two-step process is observed during the binding of sarcosine or MTA to wild-type MSOX where an initially formed complex undergoes a conformational change to form a more stable complex (*12*).

What Is the Role of Lys265 in Oxygen Activation? Substitution of Lys265 by a neutral residue yields mutants which reduce oxygen at rates that are about 10-fold slower than observed for the reaction with free reduced flavin. The results show that the 1000-fold rate acceleration observed for the reaction with wild-type MSOX can be assigned to a single positively charged amino acid residue. The observed

rate acceleration must be achieved by decreasing the activation energy for the initial 1-electron transfer step that produces a flavin/superoxide anion radical pair, the rate-determining step in the reaction of reduced flavins with molecular oxygen (*1–4, 31*). The activation energy for the 1-electron transfer step will be depend on the free energy change (ΔG°) and the reorganization energy (λ) (eq 2) (*34*).

$$\Delta G^{\ddagger} = (\lambda + \Delta G^\circ)^2/4\lambda \quad (2)$$

ΔG° is directly proportional to the reduction potential difference between the two half-reactions (ΔE°). The reorganization energy is the energy required to convert from reactant to product state in the absence of electron transfer and contains contributions from the energy required to change bond lengths and angles (λ_{in}) and the energy required to change the configuration of the surrounding medium (λ_{out}). The positively charged ϵ-amino group of Lys265 might activate oxygen by increasing the 1-electron reduction potential for the $O_2/O_2^{\bullet-}$ couple ($E^\circ = -160$ mV vs NHE), similar to the effect observed with cations in model studies (*35*). However, the kinetics observed for the self-exchange reaction between oxygen and superoxide anion indicate that λ_{out} constitutes the major energy barrier in the 1-electron reduction of oxygen (*36*). Importantly, the region above the *si*-face of FAD in MSOX contains a pair of water molecules that are sandwiched between flavin N(5) and the positively charged ϵ-amino group of Lys265 (Figure 1). The identification of Lys265 as the site of oxygen activation strongly suggests that the solvent molecules might define a preorganized binding site for superoxide anion that could accelerate the 1-electron reduction of oxygen by lowering the reorganization energy associated with transforming the surrounding medium (λ_{out}). The model implies that at least one of the water molecules is replaced by oxygen and that superoxide formation occurs in the pocket defined by one or both of these solvent molecules. A channel that might serve to transport oxygen from the protein surface to the postulated superoxide binding site is not detected in the crystal structure, suggesting that oxygen may gain access via dynamic protein fluctuations, as proposed for the rapid diffusion of oxygen through myoglobin (*37*). The substantial decrease in oxygen reactivity observed with the Lys265Arg mutant (250-fold) suggests that substitution of Lys265 with a somewhat larger basic residue may cause subtle changes in the local environment that have a major effect on the putative superoxide anion binding site. Indeed, substitution of a glycine near the N(5)−C(4a) locus of the flavin in lactate monooxygenase with alanine results in a 100-fold decrease in the rate of the reaction of the reduced enzyme with oxygen (*38*).

Concluding Remarks. Oxygen activation by MSOX exhibits a number of similarities with results obtained for the reaction with glucose oxidase. A single basic residue, Lys265 or His516, respectively, has been identified as the site of oxygen activation in each enzyme. Lys265 in MSOX and His516 in glucose oxidase are located near the N(5)−C(4a) flavin locus and hydrogen bonded to at least 1 water molecule. The positively charged imidazole ring of His516 in glucose oxidase lowers the activation energy for oxygen reduction primarily by preorganization of the surrounding medium (λ_{out}) (*2–4*), similar to the role postulated for the positively charged ϵ-amino group of Lys265 in MSOX. Lys265 is conserved or substituted by a histidine in various MSOX homologues, including *N*-methyltryptophan oxidase, pipecolate oxidase and fructosyl amino acid oxidase (*17, 18, 23, 24*), suggesting that a single basic residue will be responsible for oxygen activation by these amino acid oxidases. Puzzlingly, Lys265 is neither conserved nor conservatively substituted in nikD, an enzyme that exhibits significant sequence (22% identity) and structural (rmsd = 1.8 Å) similarity with MSOX. However, it is worth noting that nikD contains a mobile cation-binding loop that has no equivalent in other members of the MSOX family (*15*). Monoamine oxidase B, polyamine oxidase, monoamine oxidase A, and L-amino acid oxidase contain a lysine residue that is hydrogen bonded to flavin N(5) via a bridging water molecule (*25–28*), similar to that observed for Lys265 in MSOX. To our knowledge, the role of these lysine residues in oxygen activation is largely unknown. However, it has been reported the Lys296Gln mutant of monoamine oxidase B does not exhibit any detectable enzyme activity (*39*). The active sites for oxygen activation and substrate oxidation in MSOX are located on opposite faces of the flavin ring (*si*- and *re*-face, respectively). In glucose oxidase both active sites are found on the *si*-face. The arrangement observed in MSOX may facilitate oxygen access to the flavin in the reduced enzyme•imine complex by avoiding the steric crowding on the *re*-face due to the presence of imine bound above the reactive N(5)−C(4a) locus. A similar dichotomy of function is not necessary in glucose oxidase where the free reduced enzyme is the species that reduces oxygen. The results obtained with MSOX suggest that separate active sites for oxygen activation and substrate oxidation may be found in other flavoprotein oxidases, especially in those enzymes where oxygen reacts with a reduced enzyme•product complex. Interestingly, an anion binding cavity and a putative oxygen channel are found on the side of the flavin that is opposite to the substrate-binding site in vanillyl-alcohol oxidase and alditol oxidase, respectively (*40, 41*), enzymes that exhibit a ternary complex mechanism. The active site for oxygen activation in MSOX was identified by structural comparison with the homologous but oxygen-unreactive FAD site in the β-subunit of TSOX. A similar approach failed to identify the basis for enormous differences in oxygen reactivity observed with lactate monooxygenase, glycolate oxidase and flavocytochrome b_2, indicating that there is still much to be learned about the mechanism of oxygen activation by flavoprotein oxidases.

SUPPORTING INFORMATION AVAILABLE

Reductive half-reaction of Lys265Met with 1.0 mM unlabeled sarcosine (Figure S1), reductive half-reaction of Lys265Met with 140 mM [N-methyl-D_3]-sarcosine (Figure S2). This material is available free of charge via the Internet at http://pubs.acs.org.

REFERENCES

1. Massey, V. (1994) Activation of molecular oxygen by flavins and flavoproteins. *J. Biol. Chem. 269*, 22459–22462.
2. Klinman, J. P. (2007) How do enzymes activate oxygen without inactivating themselves? *Acc. Chem. Res. 40*, 325–333.
3. Roth, J. P., and Klinman, J. P. (2003) Catalysis of electron transfer during activation of O_2 by the flavoprotein glucose oxidase. *Proc. Natl. Acad. Sci. U.S.A. 100*, 62–67.

4. Roth, J. P., Wincek, R., Nodet, G., Edmondson, D. E., McIntire, W. S., and Klinman, J. P. (2004) Oxygen isotope effects on electron transfer to O_2 probed using chemically modified flavins bound to glucose oxidase. *J. Am. Chem. Soc. 126*, 15120–15131.
5. Wagner, M. A., Khanna, P., and Jorns, M. S. (1999) Structure of the flavocoenzyme of two homologous amine oxidases: Monomeric sarcosine oxidase and N-methyltryptophan oxidase. *Biochemistry 38*, 5588–5595.
6. Wagner, M. A., Trickey, P., Chen, Z., Mathews, F. S., and Jorns, M. S. (2000) Monomeric sarcosine oxidase: 1. Flavin reactivity and active site binding determinants. *Biochemistry 39*, 8813–8824.
7. Wagner, M. A., and Jorns, M. S. (2000) Monomeric sarcosine oxidase: 2. Kinetic studies with sarcosine, alternate substrates and a substrate analogue. *Biochemistry 39*, 8825–8829.
8. Hassan-Abdallah, A., Bruckner, R. C., Zhao, G., and Jorns, M. S. (2005) Biosynthesis of covalently bound flavin: Isolation and in vitro flavinylation of the monomeric sarcosine oxidase apoprotein. *Biochemistry 44*, 6452–6462.
9. Hassan-Abdallah, A., Zhao, G., and Jorns, M. S. (2006) Role of the covalent flavin linkage in monomeric sarcosine oxidase. *Biochemistry 45*, 9454–9462.
10. Hassan-Abdallah, A., Zhao, G., and Jorns, M. S. (2008) Covalent flavinylation of monomeric sarcosine oxidase: Identification of a residue essential for holoenzyme biosynthesis. *Biochemistry 47*, 1136–1143.
11. Trickey, P., Wagner, M. A., Jorns, M. S., and Mathews, F. S. (1999) Monomeric sarcosine oxidase: Structure of a covalently-flavinylated secondary amine oxidizing enzyme. *Structure 7*, 331–345.
12. Zhao, G., and Jorns, M. S. (2006) Spectral and kinetic characterization of the Michaelis charge transfer complex in monomeric sarcosine oxidase. *Biochemistry 45*, 5985–5992.
13. Khanna, P., and Jorns, M. S. (2001) N-Methyltryptophan oxidase from *Escherichia coli*: Reaction kinetics with N-methyl amino acid and carbinolamine substrates. *Biochemistry 40*, 1441–1450.
14. Dodt, G., Kim, D. G., Reimann, S. A., Reuber, B. E., McCabe, K., Gould, S. J., and Mihalik, S. J. (2000) L-pipecolic acid oxidase, a human enzyme essential for the degradation of L-pipecolic acid, is most similar to the monomeric sarcosine oxidases. *Biochem. J. 345*, 487–494.
15. Carrell, C. J., Bruckner, R. C., Venci, D., Zhao, G., Jorns, M. S., and Mathews, F. S. (2007) NikD, an unusual amino acid oxidase essential for nikkomycin biosynthesis: Structures of closed and open forms at 1.15 and 1.90 Å resolution. *Structure 15*, 928–941.
16. Venci, D., Zhao, G., and Jorns, M. S. (2002) Molecular characterization of nikD, a new flavoenzyme important in the biosynthesis of nikkomycin antibiotics. *Biochemistry 41*, 15795–15802.
17. Wu, X., Takahashi, M., Chen, S. G., and Monnier, V. M. (2000) Cloning of the Amadoriase I isoenzyme from *Aspergillus sp.*: Evidene of FAD covalently linked to Cys342. *Biochemistry 39*, 1515–1521.
18. Miura, S., Ferri, S., Tsugawa, W., Kiin, S., and Sode, K. (2006) Active site analysis of fructosyl amine oxidase using homology modeling and site-directed mutagenesis. *Biotechnol. Lett. 28* 1895–1900.
19. Chen, Z., Hassan-Abdallah, A., Zhao, G., Jorns, M. S., and Mathews, F. S. (2006) Heterotetrameric sarcosine oxidase: Structure of a diflavin metalloenzyme at 1.85 Å resolution. *J. Mol. Biol. 360*, 1000–1018.
20. Jorns, M. S. (1985) Properties and catalytic function of the two nonequivalent flavins in sarcosine oxidase. *Biochemistry 24*, 3189–3194.
21. Kvalnes-Krick, K., and Jorns, M. S. (1986) Bacterial sarcosine oxidase: Comparison of two multisubunit enzymes containing both covalent and noncovalent flavin. *Biochemistry 25*, 6061–6069.
22. Willie, A., Edmondson, D. E., and Jorns, M. S. (1996) Sarcosine oxidase contains a novel covalently bound FMN. *Biochemistry 35*, 5292–5299.
23. Ilari, A., Bonamore, A., Franceschini, S., Fiorillo, A., Boffi, A., and Colotti, G. (2008) The X-ray structure of N-methyltryptophan oxidase reveals the structural determinants of substrate specificity. *Proteins 71* 2065–2075.
24. Reuber, B. E., Karl, C., Reimann, S. A., Mihalik, S. J., and Dodt, G. (1997) Cloning and functional expression of a mammalian gene for a peroxisomal sarcosine oxidase. *J. Biol. Chem. 272*, 6766–6776.
25. Binda, C., Li, M., Hubalek, F., Restelli, N., Edmondson, D. E., and Mattevi, A. (2003) Insights into the mode of inhibition of human mitochondrial monoamine oxidase B from high-resolution crystal structures. *Proc. Natl. Acad. Sci. U.S.A. 100*, 9750–9755.
26. Binda, C., Coda, A., Angelini, R., Federico, R., Ascenzi, P., and Mattevi, A. (1999) A 30 angstrom long U-shaped catalytic tunnel in the crystal structure of polyamine oxidase. *Structure 7*, 265–276.
27. Son, S., Ma, J., Kondou, Y., Yoshimura, M., Yamashita, E., and Tsukihara, T. (2008) Structure of human monoamine oxidase A at 2.2-Å resolution: The control of opening the entry for substrates/inhibitors. *Proc. Natl. Acad. Sci. U.S.A. 105*, 5739–5744.
28. Pawelek, P. D., Cheah, J., Coulombe, R., Macheroux, P., Ghisla, S., and Vrielink, A. (2000) The structure of L-amino acid oxidase reveals the substrate trajectory into an enantiomerically conserved active site. *EMBO J. 19*, 4204–4215.
29. Ho, S. N., Hunt, H. D., Horton, R. M., Pullen, J. K., and Pease, L. R. (1989) Site-directed mutagenesis by overlap extension using the polymerase chain reaction. *Gene 77*, 51–59.
30. Hassan-Abdallah, A., Zhao, G., Chen, Z., Mathews, F. S., and Jorns, M. S. (2008) Arg49 is a bifunctional residue important in catalysis and biosynthesis of monomeric sarcosine oxidase: A context-sensitive model for the electrostatic impact of arginine to lysine mutations. *Biochemistry 47*, 2913–2922.
31. Mattevi, A. (2006) To be or not to be an oxidase: challenging the oxygen reactivity of flavoenzymes. *TIBS 31*, 276–283.
32. Basran, J., Bhanji, N., Basran, A., Nietlispach, D., Mistry, S., Meskys, R., and Scrutton, N. S. (2002) Mechanistic aspects of the covalent flavoprotein dimethylglycine oxidase of *Arthrobacter globiformis* studied by stopped-flow spectrophotometry. *Biochemistry 41*, 4733–4743.
33. Ghisla, S., Massey, V., Lhoste, J. M., and Mayhew, S. G. (1974) Fluorescence and optical characteristics of reduced flavines and flavoproteins. *Biochemistry 13*, 589–597.
34. Marcus, R. A., and Sutin, N. (1985) Electron transfers in chemistry and biology. *Biochim. Biophys. Acta 811*, 265–322.
35. Sawyer, D. T. (1991) *Oxygen chemistry*, Oxford University Press, New York.
36. Lind, J., Shen, X., Merenyi, G., and Jonsson, B. O. (1989) Determination of the rate constant of self-exchange of the $O_2/O_2^{\bullet-}$ couple in water by $^{18}O/^{16}O$ isotope marking. *J. Am. Chem. Soc. 111*, 7654–7655.
37. Brunori, M., Bourgeois, D., and Vallone, B. (2004) The structural dynamics of myoglobin. *J. Struct. Biol. 147*, 223–234.
38. Sun, W., Williams, C. H. J., and Massey, V. (1996) Site-directed mutagenesis of glycine 99 to alanine in L-lactate monooxygenase from *Mycobacterium smegmatis*. *J. Biol. Chem. 271*, 17226–17233.
39. Kacar, B., and Edmondson, D. E. (2006) Studies on the role of lysine-296 in human mitochondrial monoamine oxidase B catalysis. *FASEB J. 20*, A478−A479.
40. Mattevi, A., Fraaije, M. W., Mozzarelli, A., Olivi, L., Coda, A., and Vanberkel, W. J. H. (1997) Crystal structures and inhibitor binding in the octameric flavoenzyme vanillyl-alcohol oxidase; The shape of the active site cavity controls substrate specificity. *Structure 5*, 907–920.
41. Forneris, F., Heuts, D. P. H. M., Delvecchio, M., Rovida, S., Fraaije, M. W., and Mattevi, A. (2008) Structural analysis of the catalytic mechanism and stereo selectivity in *Streptomyces coelicolor* alditol oxidase. *Biochemistry 47*, 978–985.
42. Zhao, G., Song, H., Chen, Z., Mathews, F. S., and Jorns, M. S. (2002) Monomeric sarcosine oxidase: Role of histidine 269 in catalysis. *Biochemistry 41*, 9751–9764.

BI8008642